



# OPEN Multi-scale modeling and simulation of skeletal muscles with different fatigue degrees based on microphysiology

Monan Wang<sup>1✉</sup>, Daixin Jin<sup>1</sup>, Haibin Wang<sup>2</sup>, Xinyi Xu<sup>1</sup> & Siyuan Zheng<sup>1</sup>

The ability for skeletal muscle to constantly generate force is limited by the muscle fatigue. The calcium ion plays a significant role of the cross-bridge cycle under fatigue conditions in the force generation of skeletal muscle. To uncover complicated fatigue behavior, we conducted a multi-scale model of skeletal muscle based on cellular biochemical events. We also parameterized our model to obtain the characteristics of the change of concentration of phosphate ions and phosphate compounds in the myoplasm. The results provided evidence that under different fatigue levels, the peak of muscle strength decreases with the increase of muscle fatigue, which proves that the synergistic effect of muscle filaments and phosphate will affect the circulation of calcium ions, thereby affecting muscle fatigue and generation of muscle force. We used our modeling approach to bring new insights into the effect of phosphate ions and synergistic effect of myofilaments.

**Keywords** Skeletal muscle, Multi-scale, Phosphate dynamics, Calcium dynamics

The muscle response is strongly associated with cell characteristics such as transmembrane ion movement, calcium ions cycle, the concentrations of metabolites, the cross-bridge dynamics and the muscle fatigue<sup>1,2</sup>. Muscle fatigue, which has been widely reported in the late literature, is particularly complex among these factors and is responsible for many of the intracellular processes that arise. Modeling of skeletal muscle behavior has typically focused on simplified phenomenological relationships or subcellular processes in semimuscular segments, according to Rohrlé et al. Huxley's (1957) two-state model initially simulated interactions between actin and myosin filaments. Although the model reflected good results under the perspective of mechanical, later studies found that cross-bridge connections occurred at different stages to achieve release results and transient dynamic responses<sup>3</sup>. To model skeletal muscle at multiple scales, it is important to consider not only the role of mechanical regulation, but also the microphysiological environment and physiological characteristics in a comprehensive manner. And Hernández-Gascón et al. combined the continuous mechanical muscle model with the phenomenological model of the excitation-contraction coupling pathway in 2013. The entire modeling framework is easy to expand and can include additional biophysical details or physiological assumptions. Weichert et al. also adopted a similar modeling method, in addition to considering the spatial propagation of action potentials<sup>4</sup>. However, this model still fails to fully simulate real biological scenarios, and at the same time fails to address the problems associated with independent motor units. Fuglevand et al. considered the actual volume of the muscles and pre-determined the preparation time of the motion unit, but the problem was that only one-way coupling and phenomenological models were used, which made the model results deviate from the actuality<sup>5</sup>. Rohrlé et al. established a two-way coupling model of a multi-scale chemical-electromechanical muscle model, which more carefully and comprehensively considered the influence of microscopic mechanisms on the model.

Recently, there have been many contributions or achievements regarding multi-scale studies in the field of skeletal muscles. For example, the results of Axel J. Fenwick et al. published in 2021 suggest that these load-dependent trajectories preserved throughout skeletal muscle (at rest) as the muscle length changes can intrinsically regulate the amount of energy produced by force. If similar phenomena remain during dynamic length changes, this multiscale mechanism of muscle function may intrinsically regulate muscle efficiency during normal physiological activity<sup>6</sup>. In 2022, Benjamin Maier et al. created a muscle-tendon complex model

<sup>1</sup>College of Mechanical and Electrical Engineering, Northeast Forestry University, Harbin, China. <sup>2</sup>Key Laboratory of Medical Biomechanics and Materials of Heilongjiang Province, Harbin University of Science and Technology, Harbin, China. ✉email: qqwmnan@163.com

of the biceps muscle that incorporates a multi-scale biophysical chemo-electro-mechanical model, which they enriched with dynamic simulations rather than the previous quasi-static continuum mechanics formulation<sup>7</sup>. Yesid Villota-Narvaez et al., in 2022 developed a multiscale mechano-biological model through an exercise training program that predicts how the protein content of muscle evolves<sup>8</sup>. Through their research, they have found that the 'activation' required for strength changes occurs during training, and that this change in 'activation' can be considered a quantitative indicator of training recommendations regarding intensity and load increases. The multiscale chemical-mechanical model proposed by Mina Karamia et al. in 2023, which raises the possibility of the stimulation of the abdominal wall muscles through calcium signaling, which may be related to the electrical activity of tissues<sup>9</sup>. Their proposed multiscale chemical-mechanical material model can predict the active response of skeletal muscle by real electromyography. Xueying Zhou et al. in 2023 proposed a MMA-Net based transverse musculoskeletal ultrasound image analysis method, which solved the problems regarding anomaly classification and cross-sectional area acquisition of transverse muscular ultrasound images, which was implemented by employing a multi-scale model that reduces the cost of training multiple neural networks, and the incorporation of the multi-scale feature fusion and other factors in the model extends the shared network layer's perceptual domain and enhances the feature extraction capability of the network<sup>10</sup>. In 2024, Zhang, Mingxia et al. introduced a multi-stage fusion segmentation model (MSF-Net) to accurately extract muscle tendon membranes and bundles from ultrasound images, which ultimately allowed for results similar to those measured manually by clinical experts, enabling the accurate extraction of muscle morphology parameters and guiding rehabilitation training, and providing a complementary imaging tool for the clinical assessment of muscle structure and function<sup>11</sup>. Benjamin Maier et al. in 2024 proposed OpenDiHu, an open-source framework for high-performance computing, which can simulate skeletal muscle in a detailed and systematic way, as well as solving multiscale models, which include measurable three-dimensional muscle mechanics, action potentials, electromyographic signals, and other signals in muscle tissue propagation, and other processes, and moreover can provide a comprehensive simulation setup for the whole system<sup>12</sup>.

Hassan et al. established a multi-scale model of continuous mechanics based on micro-mechanism in 2018. The model fused the cross-bridge cycle model with the thermodynamic model to analyze the relationship between calcium ions and muscle fatigue<sup>13</sup>. The prediction results agreed with the experimental results to a great extent. But due to many influencing factors, the researchers ignored the influence of pH value, phosphate ion, temperature, synergistic effect of myofilaments, and other factors on muscle fatigue in the modeling process<sup>14</sup>. Therefore, a multi-scale model of skeletal muscle based on the micro-physiological mechanism considering the actual influence of the synergistic effect of myofilament and phosphate ions based on Hassan et al.'s model is established in this work. First, by analyzing the influence of the accumulation of inorganic phosphate produced by muscle filament movement on the calcium ion cycle, an energy metabolism model is established based on the micro-physiological mechanism of muscle fibers to complete the overall model. Then synergistic effect of myofilaments on the cross-bridge circulation is added, and a cross-bridge circulation model dominated by calcium ions is established. Finally, the established models are simulated through the MATLAB, and the simulation results are compared with classic experiments and other similar models<sup>15–18</sup>. The characteristics of the concentration change of phosphate ion in the process of generating muscle force, the relationship of muscle force and calcium ion concentration and the output change of muscle force under fatigue are obtained.

## Materials and methods

Our model of action potentials in mammalian skeletal muscle fibers describes membrane currents in the sarcolemma and t-tubules. The model includes descriptions of an inward rectifier current, a delayed rectifier current in both the sarcolemma and t-tubules<sup>19</sup>. Calcium ions are assumed to be passively distributed across the membrane according to a Donnan equilibrium. Although electroneutral ion transporters such as the NKCC and NCC cotransporters contribute to the resting membrane potential and generic mathematical models of these channels have been constructed, for simplicity, we include electroneutral transport terms in our model to ensure constant ionic gradients at the resting membrane potential<sup>20</sup>.

The mechanical environment inside the human body is extremely complicated, as a result, simple research method has great limitations when studying properties of skeletal muscles. But why we need multi-scale modeling method? When the modeling object is a complicated integrated system which widely ranges from multiple temporal and spatial scales, it was often modeled at a single scale<sup>21</sup>. Though it is simplified, but if analyzed from a higher scale, it will be accurate in quantity. To obtain holistic and integrative understanding of the working mechanism of skeletal muscle, we should study them across two or more scales, including temporal and spatial scales. Temporal scales range from seconds to months, which could be as short as the time of an electromyographic signal and also could be as long as the time of an entire healing process of injured muscles<sup>22</sup>. Spatial scales include molecule scale, subcellular scale, cellular scale, tissue scale, organ scale, system scale and entire human body scale. The binding of myoplasmic  $\text{Ca}^{2+}$  to troponin on the myofilaments generates cross-bridge cycling and force generation<sup>23–25</sup>. We have constructed an 8-state model of the XB dynamics in skeletal muscle that is based on existing generic models of XB cycling. In skeletal muscle two  $\text{Ca}^{2+}$  ions must bind to the troponin-tropomyosin regulatory unit (RU) to switch it from a position that blocks to a position that permits myosin binding and cross-bridge cycling kinetics<sup>26</sup>. Once the tropomyosin block is removed the detached XB can move to a state where the myosin head is attached pre-power stroke, a state where the myosin head is attached post-power stroke before returning to the detached state<sup>27</sup>. When decreases to basal levels the  $\text{Ca}^{2+}$  ions unbind from the RU and the XB returns to the resting detached state. Transitions between these states are modelled using first order kinetics. Our minimal scheme for XB cycling. Metabolic fatigue refers to the effect of metabolic changes on the contractile process. A number of metabolic changes occur during repeating muscle contraction such as decreasing ATP and pH and increasing phosphate and ADP<sup>28,29</sup>. In mammalian tissue acidification has little effect on isometric force.

Phosphate energy supply system is an instant energy supply system in the human body. It mainly uses creatine kinase to hydrolyze creatine phosphate through a chemical reaction, transfers the energy obtained from the decomposition of high-energy phosphate bonds to ADP, and then synthesizes ATP required for physiological activities<sup>30</sup>. The advantage of the phosphate system is that it produces ATP at a rapid rate and can support the energy required for high-intensity activities in a short period of time. This is one of the important elements that determine the explosive power of the human body. However, the content of PCR in the human body is very small, so the ATP produced is very limited<sup>31</sup>. It can only support high-intensity exercise of the human body for 5–10 s<sup>32</sup>. When the phosphate source energy supply system fails, the glycolytic energy supply system (also known as the short-term energy system) will continue to synthesize ATP to help the body continue the contraction-diastole movement of skeletal muscle fibers<sup>33</sup>. The energy supply process of glycolysis is mainly the decomposition of muscle glycogen under anaerobic conditions to provide energy for the synthesis of ATP, but this process will be accompanied by the production of lactic acid, which will be rapidly decomposed into lactate and hydrogen ions<sup>29</sup>. With the accumulation of lactic acid in the human body, the activity of the key catalytic enzyme involved in the reaction gradually decreases, and the reaction rate decreases accordingly, and the glycolysis system provides less and less energy for the synthesis of ATP. In skeletal muscle contraction exercises, high concentrations of hydrogen ions will produce acidic burning and soreness, leading to premature muscle fatigue<sup>34–36</sup>. Both of these energy supply systems are anaerobic energy metabolism systems that support high-intensity and short-term exercise.

When the human body is doing non-strenuous exercise, the main energy supply system is the aerobic breathing energy supply system (also known as oxidative phosphorylation). Its advantage is that it can generate a large amount of ATP and support long-term activities. The disadvantage is that it requires more time for aerobic breathing. The process of oxidative phosphorylation is the process of decomposing carbon oxygen compounds such as sugars and fats into carbon dioxide and water. The energy produced provides important power for the synthesis of ATP. The process of oxidative phosphorylation occurs on the inner membrane of the mitochondria, and this structure is also called the electron transport chain<sup>32</sup>. Because a large amount of electrons and ions are generated and exchanged on it, and finally H<sub>2</sub>O and ATP are produced. Description of the three energy supply systems, as shown in Table 1.

Many physiological metabolic processes, such as glycolysis and tricarboxylic acid cycle, will produce reduced coenzyme (NADH). This coenzyme contains electrons with high electrode potential, which means that it can release a lot of energy during oxidation. Studies have confirmed that the use of extracellular reduced coenzymes affects the intracellular ATP. This phenomenon indicates that reduced coenzymes act from outside the cell to the inside of the cell. When the cell undergoes a chemical reaction, the energy during the reaction is gradually released, because if all the energy is released at once, the reaction will become uncontrollable. Therefore, electrons are released from NADH and transferred to oxygen through a series of reactions. The energy release in each step is gradual. On the inner membrane of mitochondria, protons enter the inner membrane of the cell under the action of energy to form a potential difference. The ATP synthase absorbs the energy it contains to produce ATP. NADH and NAD<sup>+</sup> are important catalysts for redox in organisms, because they act as donors of hydrogen and electrons and acceptors of hydrogen and electrons respectively in the redox process of organisms.

In the process of skeletal muscle contraction, skeletal muscle fibers will fatigue under multiple stimulations. There are many factors that cause fatigue, such as changes in ion concentration (such as H<sup>+</sup>, Pi) in muscle fibers, changes in temperature, and synergistic effects of muscle filaments, etc<sup>37–39</sup>. If all these factors are considered, it will cause great difficulties for muscle fatigue analysis and muscle strength analysis. Therefore, this article only considers the effect of phosphate in muscle fibers on muscle fatigue on the molecular scale, and considers the synergistic effect of muscle filaments on the subcellular scale.

Energy is essential in the process of skeletal muscle movement, and the main energy supply substance is ATP. In the process of decomposing ATP to produce energy, the concentration of phosphate ions in the muscle mass will continue to increase as ATP is decomposed. Although phosphate reacts with creatine kinase to generate phosphokinase to maintain the balance of phosphate ion concentration in the muscle mass, there is still a large amount of phosphate ions accumulated in the muscle mass, resulting in phosphate in the muscle mass. The concentration of phosphate continues to increase, and then part of the phosphate ions in the sarcoplasmic reticulum will enter the sarcoplasmic reticulum, making the phosphate ion concentration in the sarcoplasmic reticulum increase accordingly. Part of the phosphate ions in the sarcoplasmic reticulum react with the original calcium ions in the sarcoplasmic reticulum to form calcium phosphate precipitation, which hinders the circulation of calcium ions and causes muscle fatigue. In this work, based on the mechanism described above, a mathematical model is established for the process of phosphate hindering the calcium ion cycle, which provides a basis for the following calcium kinetic modeling.

The concentration equation is established to simulate the dynamic change process of phosphate ions in the sarcoplasm and sarcoplasmic reticulum, which helps to analyze the influence of phosphate ions on the process

Energy supply system	Reactant	Characteristic
Phosphate energy supply system	creatine phosphate	anaerobic energy metabolism systems, instant energy supply, support high-intensity and short-term exercise
glycolytic energy Supply system	muscle glycogen	support high-intensity and short-term exercise, supply mainly under anaerobic conditions, product lactic acid
aerobic breathing energy supply system	carbon oxygen compounds	generates a large amount of ATP, support long-term activities, requires more time

**Table 1.** Description of the three energy supply systems.

of muscle contraction. In addition, according to the energy cycle process in muscle fibers and the reaction mechanism of oxidative phosphorylation, a mathematical model for the synthesis of ATP with the participation of phosphate and phosphate compounds is established.

Multi-scale modelling has been used in many basic sciences such as mathematics, material science, chemistry and fluid dynamics etc. for many years. The recent years have witnessed the great development and achievement in studies of human biology, and in which, multi-scale modeling method has been playing an increasingly important role when cross-scale issues occur. In the future, multi-scale modeling method will not lose its value obviously. On the contrary, it may also plays a great role elsewhere, such as biomimetic engineering.

At present, multi-scale modeling of cardiac muscles has also been fashionable. The cardiac muscle is a very complex tissue with very important functions. It can be said that the myocardium is one of the most important organs of the organism. As a closely related biological structure to cardiac muscles, the cardiovascular system plays a crucial role in researches of cardiac muscles. In 2010, Joseph L. Greenstein et al. reviewed experimentally based multi-scale computational models of cardiac excitation-contraction coupling and some of their applications. They also pointed out that multi-scale modeling methods have revealed many mechanical relationships between interactions of different biological scales. In 2017, Fyodor A. Syomin et al. designed a suitable model of cardiac muscle which could reproduce all main properties of cardiac muscle observed in experiments with single cells in order to better conduct the multi-scale simulation of the pumping function of the heart.

Cardiac muscle and skeletal muscle are both classified into striated muscles, and they share many similarities. Some researchers study mechanical behaviors and functions of cardiac muscle and skeletal muscle together, achieving significant results. The multi-scale methods used in skeletal muscle biomechanics may also be used in clinical diagnosis, biomimetic engineering or other aspects. However, we have to admit, owing to the enormous complexity of skeletal muscle biomechanics, there are still a great deal of problems to be solved. First of all, the obtainment of individual muscle force in vivo in motions is still a huge challenge in musculoskeletal biomechanics for quite a long time to come. To consummate model parameters is a top priority. Moreover, the validation of multi-scale simulation results is also a rough task, embodied that it is complicate and time-consuming. If the efficiency could be improved by a wide margin, we may look forward to its vital role in clinical diagnosis.

## Modeling of phosphate dynamics and energy metabolism in skeletal muscles

### Dynamic modeling of phosphate in skeletal muscle fibers

Energy is essential in the exercise process of skeletal muscle, and the main energy supply substance is ATP. In the process of decomposition of ATP to produce energy, the concentration of phosphate ions in muscle mass will continuously increase with the decomposition of ATP<sup>40</sup>. Although phosphate reacts with creatine kinase to generate phosphokinase to maintain the balance of phosphate ion concentration in muscle, there are still a large amount of phosphate ions accumulated in muscle, which leads to the constant increase of phosphate concentration in muscle, and then part of phosphate ions in muscle will enter the sarcoplasmic reticulum. Thus, the concentration of phosphate ions in the sarcoplasmic reticulum also increases correspondingly<sup>41</sup>. In the sarcoplasmic reticulum, some phosphate ions react with calcium ions to form calcium phosphate precipitate, which obstructs the circulation of calcium ions and causes muscle fatigue. Based on the mechanism described above, a mathematical model of the process of phosphate blocking the circulation of calcium ions is established in this work, which provides a basis for the modeling of calcium dynamics in the following work.

In the process of ATP synthesis, phosphate provides material guarantee for the reaction. The formula for calculating the concentration of phosphate ions in mitochondria of muscle fibers is as follows:

$$\dot{P}_{ti} = (v_{PI} - v_{SN}) \cdot R_{cm} \quad (1)$$

where  $v_{PI}$  represents the reaction coefficient of phosphate carrier,  $v_{SN}$  represents the ATP synthetic coenzyme catalyzed reaction rate coefficients, and  $R_{cm}$  represents cell to mitochondria volume ratio.

The reaction coefficient of phosphate carrier is calculated as follows:

$$v_{PI} = k_{PI} \cdot (P_{ije} \cdot H_e - P_{iji} \cdot H_i) \quad (2)$$

where  $k_{PI}$  represents the phosphate reaction balance coefficient,  $P_{ije}$  represents the concentration of phosphate ions in muscle,  $H_e$  represents the concentration of hydrogen ions in muscle,  $P_{iji}$  represents the concentration of phosphate ions in mitochondria, and  $H_i$  represents the concentration of hydrogen ions in mitochondria.

The formula for calculating the change of hydrogen ion concentration in muscle mass is as follows:

$$\dot{H}_e^+ = -(2(2 + 2u)v_{C4} + 4v_{C1} - n_A v_{SN} - uv_{EX} - (1 - u)v_{PI})R_{cm}/r_{buff} \quad (3)$$

In the formula,  $u$  represents the bonding strength coefficient between hydrogen ion and carrier,  $v_{C1}$  represents the rate coefficient of ion channel complex I,  $n_A$  represents the ratio coefficient between hydrogen ion and ATP in ATPase reaction,  $v_{EX}$  represents ATP/ADP carrier rate coefficient, and  $r_{buff}$  represents the buffer capacity coefficient of hydrogen ion.

The formula for calculating the ion flux rate coefficient of ion channel complex IV on the inner mitochondrial membrane is:

$$v_{C4} = k_{C4} \cdot \frac{1}{1 + K_{mO}/O_2} \quad (4)$$

where  $k_{C4}$  represents complex IV flux coefficient,  $K_{mO}$  represents rate coefficient of oxygen transport in muscle fibers, and  $O_2$  represents oxygen concentration.

The formula for calculating the concentration of phosphate ions produced by hydrolysis of ATP in muscle mass is:

$$\dot{P}_S = v_{UT} - v_{PI} \quad (5)$$

where  $v_{UT}$  represents the coefficient of ATP consumption rate in muscle mass.

The formula for calculating the concentration of ATP produced by mitochondria and transported to muscle is:

$$\dot{ATP}_{te} = v_{EX} - v_{UT} + v_{AK} + v_{CK} \quad (6)$$

Where  $v_{AK}$  represents adenylate kinase catalytic reaction coefficient, and  $v_{CK}$  represents creatine kinase catalytic reaction coefficient.

The formula for calculating the catalytic reaction coefficient of adenylate kinase is:

$$v_{AK} = k_{AK} \cdot ADP_{fe} \cdot ADP_{me} - k_{bAK} \cdot ATP_{me} \quad (7)$$

where  $k_{AK}$  is the reaction equilibrium coefficient catalyzed by adenylate kinase,  $ADP_{fe}$  represents the concentration of free ADP in the muscle mass,  $ADP_{me}$  represents the concentration of ADP in sarcoplasmic that binds to magnesium ions,  $k_{bAK}$  is the negative feedback equilibrium coefficient catalyzed by adenylate kinase, and  $ATP_{me}$  represents the concentration of ATP in sarcoplasmic that binds to magnesium ions.

There is a negative linear correlation between the concentration change rate of phosphocreatine and the catalytic reaction coefficient of creatine kinase. The formula for calculating the catalytic reaction coefficient of creatine kinase is:

$$v_{CK} = k_{fCK} \cdot ADP_{te} \cdot PCr \cdot H_e^+ - k_{bCK} \cdot ATP_{te} \cdot Cr \quad (8)$$

where  $k_{fCK}$  represents the balance coefficient of the reaction catalyzed by creatine kinase,  $ADP_{te}$  represents the total concentration of ADP in sarcoplasmic,  $k_{bCK}$  is the negative feedback equilibrium coefficient catalyzed by creatine kinase,  $ATP_{te}$  represents the total concentration of ATP in sarcoplasmic, and  $Cr$  represents the concentration of creatine in muscle fibers. The parameters in the above model were determined by consulting the model parameters developed by Korzeniewski et al.<sup>42,43</sup>.

This concentration equation simulates the dynamic changes of phosphate ions in the muscle and the sarcoplasmic reticulum, which is helpful to analyze the influence of phosphate ions on the muscle contraction process. In addition, according to the energy cycling process and the reaction mechanism of oxidative phosphorylation in muscle fibers<sup>44</sup>, a mathematical model of ATP synthesis reaction involving phosphate and phosphoric acid compounds was established.

### Multi-scale modeling of calcium dynamics and thermodynamics in skeletal muscle fibers

The circulation of calcium ions in muscles plays a key role in the process of contraction. The quantity and concentration changes of calcium ions in muscle fibers are the basis for regulating the balance of ion concentration in muscle fibers and initiating muscle contraction. As the second messenger, calcium ions combine the action potential with muscle fiber contraction and movement, making the muscle complete the related contraction and relaxation actions. According to the micro-physiological mechanism of calcium dynamics<sup>45</sup>, considering the influence of myofilaments synergistic effect on the cyclic motion of cross-bridge, based on the previous model, the principle of virtual work was used to establish a thermodynamic model integrated with the cross-bridge cyclic model, and complete the establishment of a multi-scale model of skeletal muscle from micro to macro.

The sarcoplasmic reticulum is a fine network channel composed of thin films, which is wrapped around the myofibrils of skeletal muscle, and its main function is to form active proteins and synthesize energy substances. The transverse tubules surrounding the myofibrils cut off the longitudinal sarcoplasmic reticulum in a regular manner, and expand on both sides of the transverse tubules to form a terminal cistern<sup>46</sup>. When the muscle contractions generate electrical signals, the nervous system transmits them to the transverse tubules, and the dihydropyridine receptors distributed on the transverse tubules can sense the voltage changes. The RYR channel (RYR) is activated by depolarization reaction<sup>47</sup>. Ryr channel is located in the sarcoplasmic reticulum, through which calcium ions can be released from the sarcoplasmic reticulum and mainly plays a role in maintaining the balance of calcium ions in muscle fibers. Both the dihydropyridine receptor and the Reynold channel have tetramer structures, as shown in Fig. 1.

The Renodine channel tetramer can form a central hole, which extends into the sarcoplasm through the part of its foot structure, making its opening toward the gap between the sarcoplasm reticulum and the transverse tubule. The top of the Renodine channel is attached to the dihydropyridine channel<sup>48,49</sup>. The voltage signal on the transverse tubule causes the conformational change of the dihydropyridine channel, and the piston on the top of the Renodine channel is removed. Calcium ions can be released from the sarcoplasmic reticulum into the sarcoplasmic tissue through the renodin channel on the endpond when it is activated and opened by the dihydropyridine receptor, as shown in Fig. 2.

When skeletal muscle fibers are in a resting state, all ions in myofibrillar fibers maintain a constant amount. Troponin in the plasmic reticulum binds a large number of calcium ions to store calcium ions, and magnesium ions in the sarcoplasm bind most of the ATP binding sites, and calcium and magnesium ions are respectively at



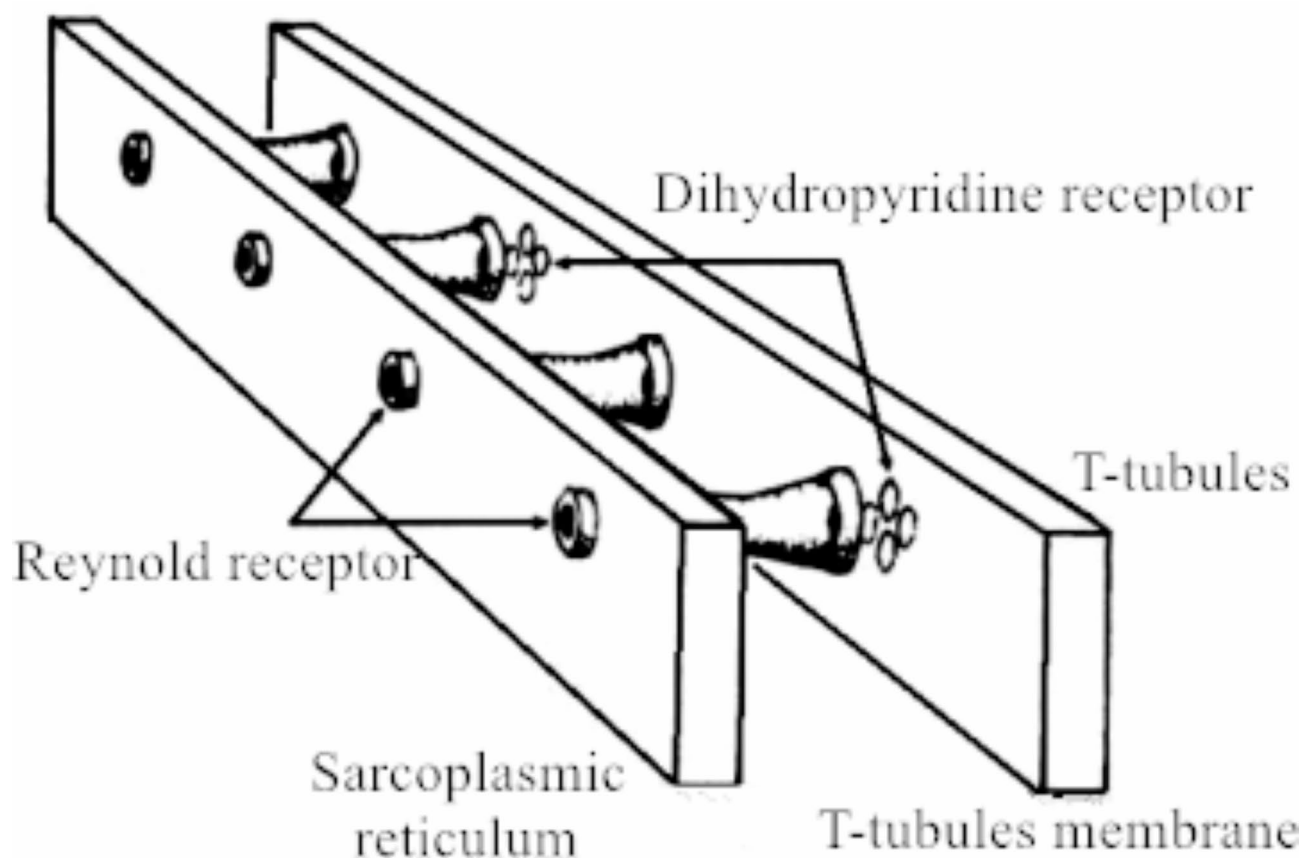


**Fig. 1.** Schematic diagram of DHPR and RYR alternate arrangement.

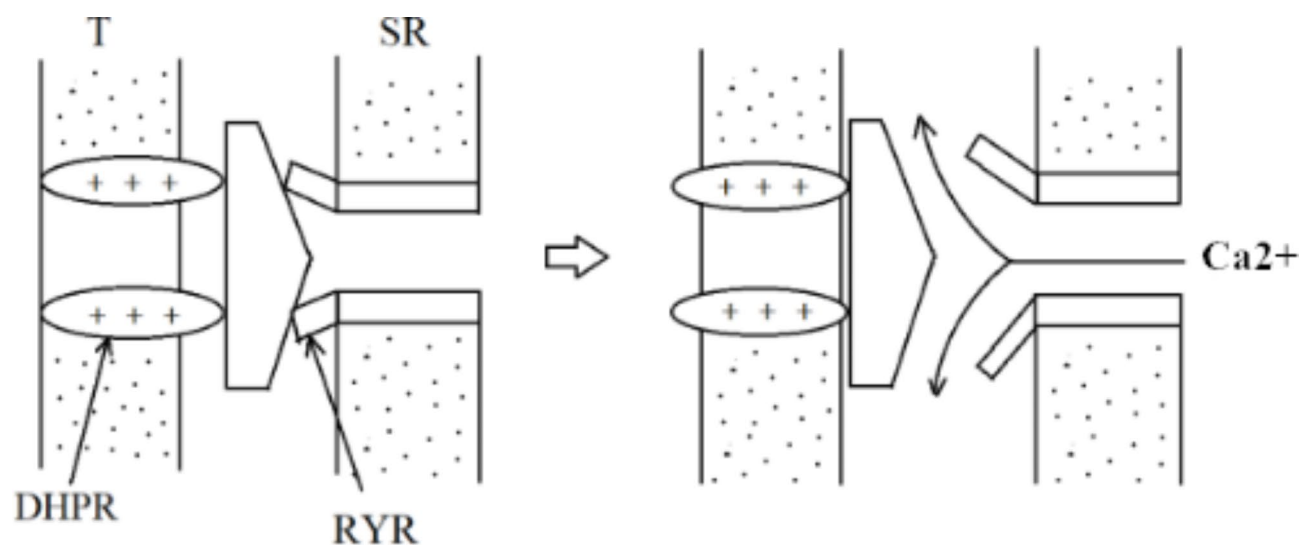


**Fig. 2.** Schematic diagram of molecular conformation changes.

the binding sites. When calcium ions enter muscle fibrocytes, part of calcium ions will bind with calmodulin, microalbumin, troponin and troponin on muscle fibrocytes, triggering conformational changes of binding proteins and activating a series of physiological and chemical reactions<sup>50</sup>.

The concentration of calcium ions in the muscle decreases as the concentration gradient transport of calcium ions goes on. At this time, calcium ions are detached from the troponin subunit C, the binding site of calcium ions on actin is re-covered by troponin, the transverse bridge link on the myofilaments is broken, and the muscle

stops contraction and returns to the diastolic state<sup>51</sup>. This completes the transport of calcium ions during muscle contraction-relaxation.

### Cross-bridge circulation in muscle fibers of skeletal muscle

The process of cross-bridge circulation is derived from the widely recognized sliding myofilament theory proposed by Aldous Huxley, which is based on the morphological characteristics of the microscopic structure of skeletal muscle and its changes during muscle contraction. The sliding myofilament theory mainly describes that when human muscles are stimulated to contract, their internal myofilament or other tangible structures will not change in shape or structure, nor will curling and shortening occur, but only through the generation of relative sliding force between thick and thin myofilament<sup>52–54</sup>. When calcium ions enter the muscle fiber, due to the increase of calcium ion concentration, there will be positive substances inside the muscle fiber to strengthen muscle, calcium ions will bind with troponin, and make tropomyosin offset. This position shift exposes the actin-myosin binding site and causes ATP to be broken down and combined with more actin to make the cross-bridge movement.

As a component of coarse muscle filaments, myosin has a special polymerization mode. The rod-shaped part is polymerized into a bundle, while the spherical part protrudes out to form a transverse bridge. This special structure enables actin to combine with the bridge conveniently and decompose ATP through related active enzymes to provide energy for the bridge activity<sup>55</sup>.

Myofilaments slide in relation to actin on them, and actin and globulin are also called contractin. Actin, tropomyosin, and troponin constitute fine myofilaments. Myosin filaments are composed of multiple myosins, and these myosin are divided into two units, each of which joins into filaments. The double helix polymerization forms the backbone of myosin filaments, while a single globulin forms a globule<sup>56</sup>. The other two proteins on the fine myofilaments are not directly involved in the interaction between the myofilaments. They mainly affect the direct binding of the contractile protein molecules, so they are called regulatory proteins.

The transverse bridge plays an important role in the process of myofilament sliding. Under certain conditions, the transverse bridge binds with actin molecules on the fine myofilaments. After the bridge binds with the myofilaments, it will move. This movement is not random and is constrained by the direction of M-line. The bridge also promotes the hydrolysis of ATP, during which the bridge is connected and moved. However, such catalysis is conditional. The bridge cannot catalyze the decomposition of ATP without limit, and it can only be catalyzed after binding with actin<sup>57</sup>. The transbridge movement will expose the actin on the fine myofilament, and the myosin on the coarse myofilament will absorb the energy of ATP decomposition into an active state and connect to the actin binding site of the fine myofilament. Then the energy generated by ATP hydrolysis will be used to pull the fine myofilament to move along the action line, that is, the M-line, towards the center of the musculobar<sup>58–60</sup>. After the completion of a transbridge connection movement, myosin is in a low energy state due to the loss of ATP. The myosin head on the coarse myofilament will break away from the actin binding site on the fine myofilament and return to the original position after the transbridge dissociation. When myosin binds with ATP molecules again, it will prepare for the next transbridge connection swing. The process of connecting, moving and disconnecting a cross-bridge is called a work stroke. Repeating the work stroke completes the cycle of the cross-bridge<sup>61–63</sup>.

The formula for calculating the concentration of calcium ion - binding troponin unit in the inner muscle fiber is as follows:

$$\frac{d[Ca^{2+}]_{TOT}}{dt} = \frac{d[Ca^{2+}]_C}{dt} + \frac{d[CaB]}{dt} + \frac{d[CaTrop]}{dt} + \frac{d[CaParv]}{dt} \quad (9)$$

The formula for calculating the concentration of calcium ions binding with buffer in muscle is as follows:

$$\frac{d[CaB]}{dt} = k_{onB}[Ca^{2+}]_C([B]_{TOT} - [CaB]) - k_{offB}[CaB] \quad (10)$$

where  $k_{onB}$  represents the reaction coefficient of calcium ion binding muscular buffer,  $[Ca^{2+}]_C$  represents the concentration of calcium ions in sarcoplasmic,  $k_{offB}$  represents the reaction coefficient of calcium ion separating muscular buffer,  $[B]_{TOT}$  represents the total concentration of muscular buffer, and  $[CaB]$  represents the complex concentration of calcium ion binding buffer.

The formula for calculating the concentration of calcium ions bound to troponin units in muscle mass is as follows:

$$\frac{d[CaTrop]}{dt} = k_{onT}[Ca^{2+}]_C([Trop]_{TOT} - [CaTrop]) - k_{offT}[CaTrop] \quad (11)$$

where  $k_{onT}$  denotes the reaction coefficient of calcium ion binding troponin,  $k_{offT}$  denotes the reaction coefficient of calcium ion separation troponin,  $[Trop]_{TOT}$  denotes the total concentration of troponin, and  $[CaTrop]$  denotes the concentration of calcin-troponin.

The formula for calculating the concentration of calcium ions binding with small albumin in muscle is as follows:

$$\frac{d[CaParv]}{dt} = k_{onCa}[Ca^{2+}]_C([Parv]_{TOT} - [CaParv] - [MgParv]) - k_{offCa}[CaParv] \quad (12)$$

where  $k_{onCa}$  represents the reaction coefficient of calcium ion binding with small albumin,  $[Parv]_{TOT}$  denotes the concentration of small albumin,  $k_{offCa}$  represents the reaction coefficient of calcium ion separation with small albumin,  $[CaParv]$  represents the concentration of calcium ion binding with small albumin, and  $[MgParv]$  represents the concentration of magnesium ion binding with small albumin.

Both magnesium and calcium ions in the muscle will compete for the binding sites of the small albumin, so a part of the small albumin will be bound by magnesium ions. In this process, the formula for calculating the concentration of magnesium ion binding small albumin is as follows:

$$\frac{d[MgParv]}{dt} = k_{onMg}[Mg^{2+}]([Parv]_{TOT} - [CaParv] - [MgParv]) - k_{offMg}[MgParv] \quad (13)$$

where  $k_{onMg}$  denotes the binding rate of magnesium ion with small albumin, and  $k_{offMg}$  denotes the separation rate of magnesium ion with small albumin. The parameters of the model developed were determined by reviewing the literature of Pizarro et al.<sup>64</sup>.

## Results

The phosphate dynamics model, the energy metabolism model, the calcium dynamics model and the thermal dynamics model were combined to simulate the multi-scale skeletal muscle model and the connecting process of the main formulas between each module. This section also compares and verifies the simulation results with those of classical experiments and other similar models, and further analyzes the changes in the concentration of key ions in the multi-scale model of skeletal muscle based on the microphysiological mechanism of skeletal muscle, the stress change characteristics of muscle contraction under different fatigue states, and the relationship between stress and contraction speed.

### Verification of phosphate kinetic model and energy metabolism model

The MATLAB platform was used to simulate the phosphate dynamics model. The relative activity of ATP represented the activation degree of ATP in muscle fibers involved in muscle fiber contraction. The relative activity of ATP was taken as the horizontal coordinate, and the concentration changes of phosphocreatine and phosphate in muscle tissue were taken as the vertical coordinate. The changes of phosphocreatine and phosphate ion concentrations in rat muscle fibers were compared with those measured by Cieslar et al.<sup>65</sup> through nuclear magnetic resonance spectroscopy and saturation correction spectroscopy, as shown in Fig. 3.

As can be seen from the figure, the change curve rates of phosphate ion concentration and phosphocreatine concentration both increased first and then slowed down. When the relative activity of ATP reached about 30%, the growth rate of phosphate ion concentration began to decrease. When the relative activity of ATP reached about 40%, the reduction rate of phosphocreatine began to decrease. This is because when muscle fibers start to contract, the relative activity of ATP use is low, and the reaction is mainly a catalytic reaction dominated by creatine kinase. With the progress of muscle fiber movement, the relative activity of ATP use gradually increases. The chemical reaction within skeletal muscle fibers is mainly based on the decomposition of creatine phosphate to produce creatine and phosphate, so the curve results in the figure are produced. Compared with the experimental results of Cieslar et al. the simulation results of creatine phosphate and phosphate ion concentration showed the same change trend, but the simulation results of creatine phosphate concentration were slightly higher than the experimental results, and the simulation results of phosphate ion concentration were slightly lower than the experimental results.

The simulation results of hydrogen ion concentration and ADP concentration were expressed by pH value (pH value is equal to the negative logarithm of hydrogen ion concentration). The obtained simulation results were compared with the experimental data of Cieslar et al., who measured the gastrocnemius muscle of rats by <sup>31</sup>P NMR spectroscopy after stimulating the gastrocnemius muscle of rats for 8–12 min. See Fig. 4.

The change of ADP concentration is positively correlated with the relative activity of ATP use, that is, ADP in muscle gradually increases with the decomposition of ATP, and its growth rate begins to decline when the relative activity of ATP use reaches about 50%, and eventually becomes flat. The simulation results of ADP concentration and pH value showed the same trend as the experimental results of Cieslar et al.

### Verification of calcium kinetic model and thermal kinetic model

MATLAB was used to simulate the relationship between muscle force, muscle filament deformation and calcium ion concentration of the mathematical model of calcium dynamics. In the simulation diagram, myofilament deformation and muscle stress under different calcium ion concentrations were studied. The abscissa was myofilament deformation, and the ordinate was the ratio of stress to minimum stress. The stress was normalized. The comparative experimental data are from the rat muscle experiment conducted by Hunter et al., and the simulation results are shown in Fig. 5. Based on the simulation results, this work analyzed the relationship between calcium ions, myofilament deformation and muscle force.

### Verification of skeletal muscle multi-scale model based on microphysiological mechanism

The comparative experimental data were obtained by Sierra et al.<sup>66</sup>, who stimulated rabbit extensor toe longus at a frequency of 100 Hz every 10s and measured the fatigue change process of rabbit extensor toe longus within one hour under the continuous stimulation time of 0.2s. In this work, four states were selected for simulation analysis, and different fatigue states were guaranteed by controlling the input concentration of calcium ions. In addition, this study also made a comparative analysis with the simulation results obtained from the cross-bridge thermodynamic model established by Mina et al.<sup>18</sup>. Firstly, muscle stress changes under non-fatigue state were simulated, and the results were shown in Fig. 6.



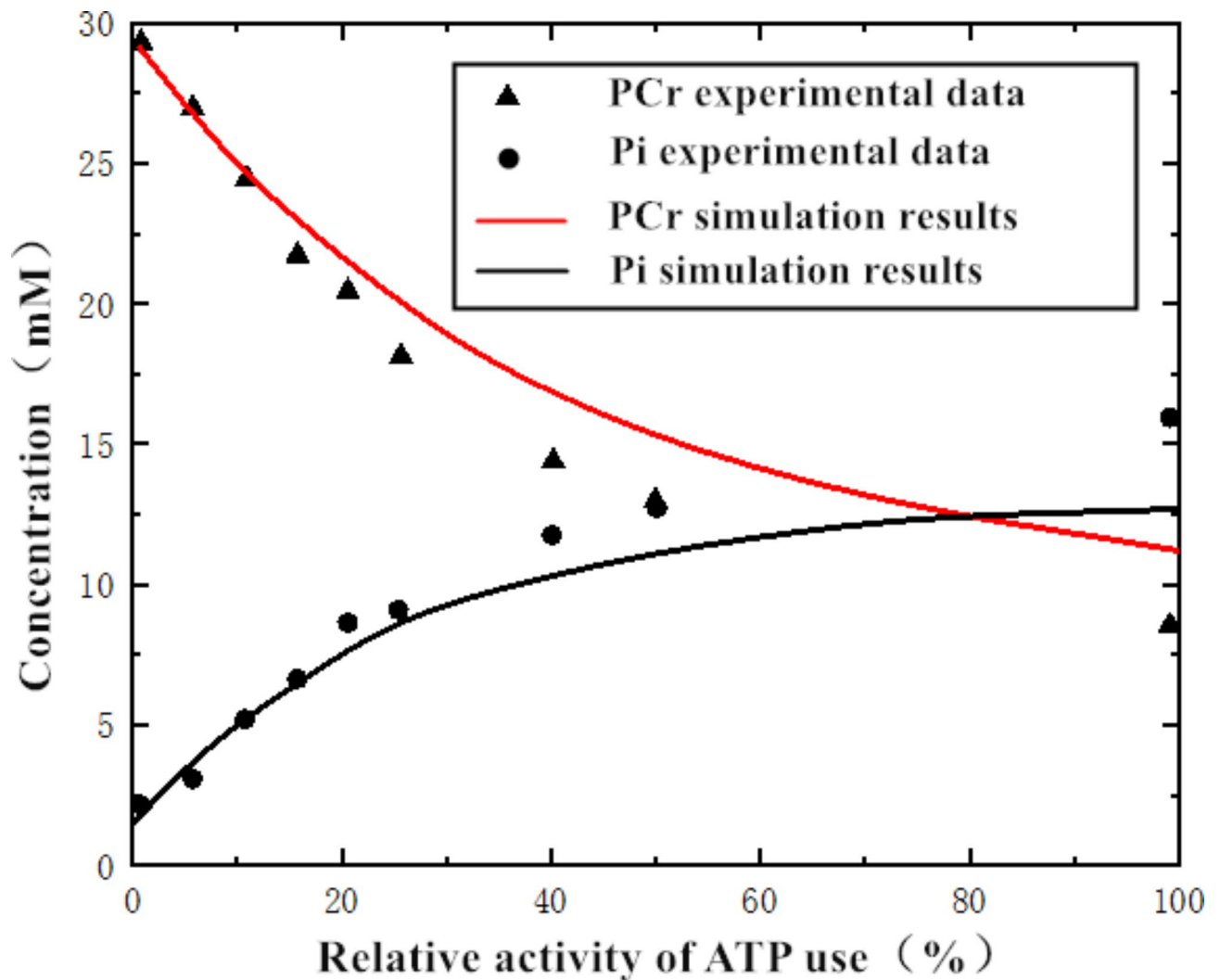


**Fig. 3.** Simulation results of PCr and Pi concentration in sarcoplasm of muscle fibers.

The muscle force peak of the model in this study is 0.421 MPa, and the relative error between it and the experimental data peak is 0.94%. The simulation result of Mina et al. is 0.435 MPa, and the relative error is 2.11%. Compared with the model proposed by Mina et al., the influence of phosphate ions on calcium ions and the synergistic effect of muscle filaments during the cross-bridge cycle was considered in this study, and the influence of temperature change and other ion concentration change in muscle mass on muscle strength was not considered.

In addition to the simulation of muscles in the non-fatigue state, this work also simulated the muscle states under the fatigue degree of 16%, 53% and 72% respectively, as shown in Figs. 7, 8 and 9, which are the simulation results under the three fatigue states respectively.

The simulation curve of the model in this study has a higher degree of fitting with the experimental data curve as it is shown in Fig. 10, which further proves the effectiveness and accuracy of the model.

Based on the above data, it can be concluded that the model proposed in this study has smaller relative errors than the model proposed by Mina et al.<sup>67</sup>, is closer to the experimental results, and has a higher degree of fitting with the actual data, which reflects the effectiveness and optimization of the model proposed in this study. This model can predict the relationship between human muscle force and muscle contraction speed, and provide a good reference analysis for actual movement.

## Discussion

There are some differences between the simulation results and the experimental results. For example, the concentration of ADP is quite different from the experimental results. The reason for the difference may be that the influence of anaerobic respiration on the chemical substances in muscle and the physiological environment is not considered, leading to the high concentration of ADP obtained by the simulation. In addition, different initial values of relevant parameters will also lead to result errors<sup>68–70</sup>. The simulation results have the same trend with the experimental results, which proves that the synergistic effect of muscle filaments does affect muscle strength.

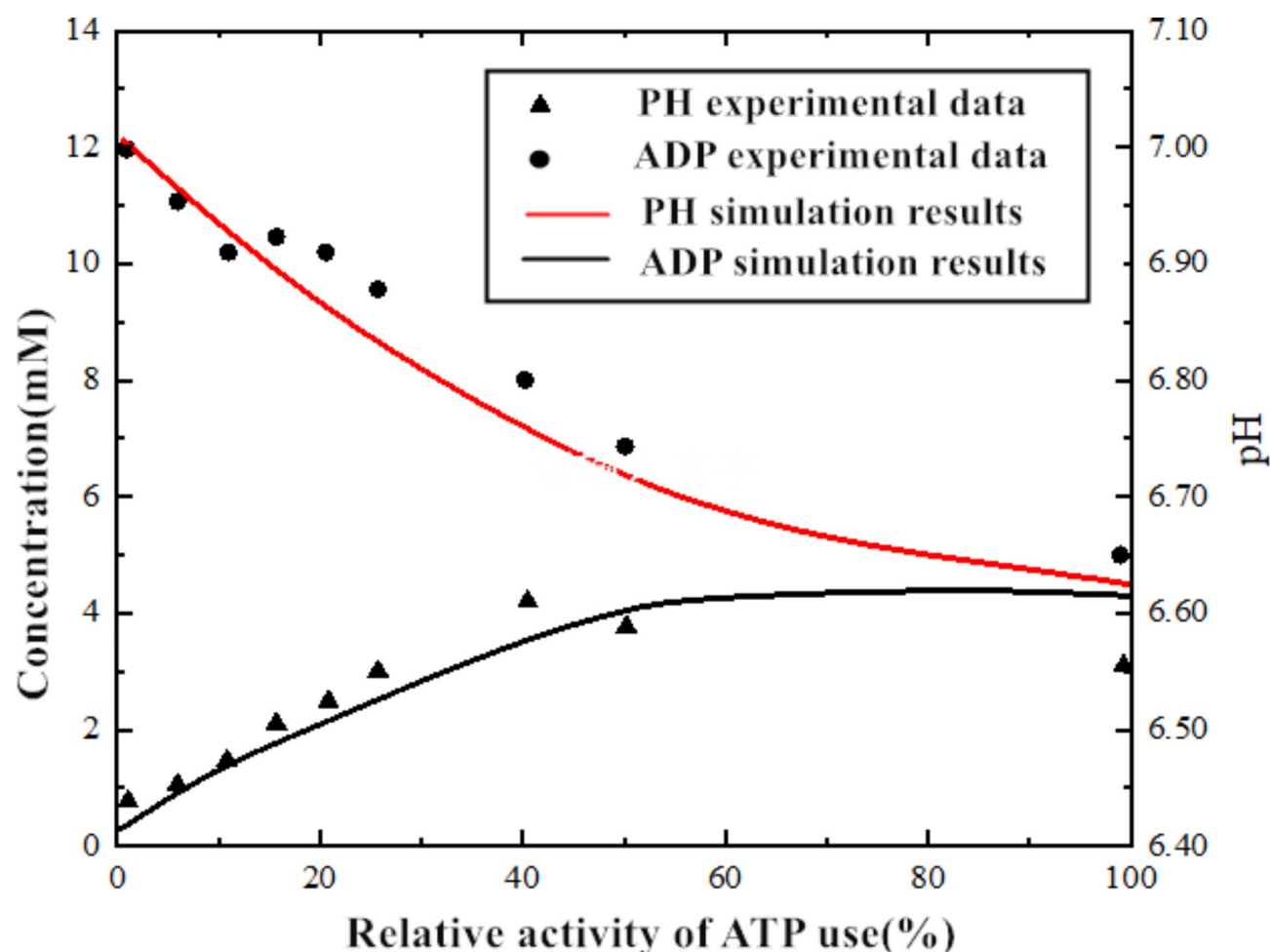


**Fig. 4.** Simulation results of pH value and ADP concentration in sarcoplasm of muscle fibers.

However, there is some data bias between the simulated curves and the experimental results, which may be caused by the fact that the model ideally considers the skeletal muscle to be in a state of non-energy dissipation, whereas some of the energy may be spilled or not taken into account, leading to data bias<sup>71</sup>. Compared with the experimental data, the stress value of the simulation results is higher when both the model and the experimental results tend to be flat in the end. The possible reason is that the influence of temperature change and other ion concentration change in muscle mass on muscle force is not considered<sup>72</sup>. With the increase of muscle fatigue degree, the peak difference of simulated stress first decreases and then increases, and the stress fitting degree decreases with the increase of fatigue degree in the same time. This is because the main research scope of this work is low-intensity exercise, which lacks correlation analysis of muscles under high fatigue conditions, and other factors affecting muscle fatigue are not considered enough<sup>73,74</sup>, such as: The effect of cell membrane on electrical signal receptor fatigue, the decrease of ionic permeability and the influence of ionic interphase during muscle fatigue can also be supplemented and expanded in the following models.

The following possible reasons are summarized: First, this model only considers the effect of phosphate ions on calcium ions, but other ions in muscle fibers, such as magnesium ions, hydrogen ions, sodium ions and potassium ions, can affect the transport of calcium ions and the generation of muscle force. Second, this work ignores the effect of temperature on muscle force contraction. Temperature change will affect the reaction rate, the binding speed and degree of ion to ion, protein to protein, and ion to protein, thus affecting the generation of muscle force. Third, this study simply considers the influence of the synergistic effect of myofilaments. Ideally, the myofilaments are considered to be in the same direction. In fact, when the myofilaments move, there is a slight Angle difference between different myofilaments, which results in the difference between the size of the resultant force and the ideal direction, which affects the expression of the final muscle force. Fourthly, electric stimulation was used to stimulate the extensor longus muscle of animals to contract in the experiment. Based on the microphysiological environment of muscle fibers, calcium ions were taken as the input parameter in this study, which led to the deviation of simulation results. These are the deficiencies of this model and the direction of further optimization of the model.

MATLAB platform was used to simulate the variation trend of phosphate and its compounds in the reaction process, the relationship between calcium ions, myofilament deformation and muscle force was analyzed, the change rule of muscle stress under different fatigue states was explored, and the relationship between stress

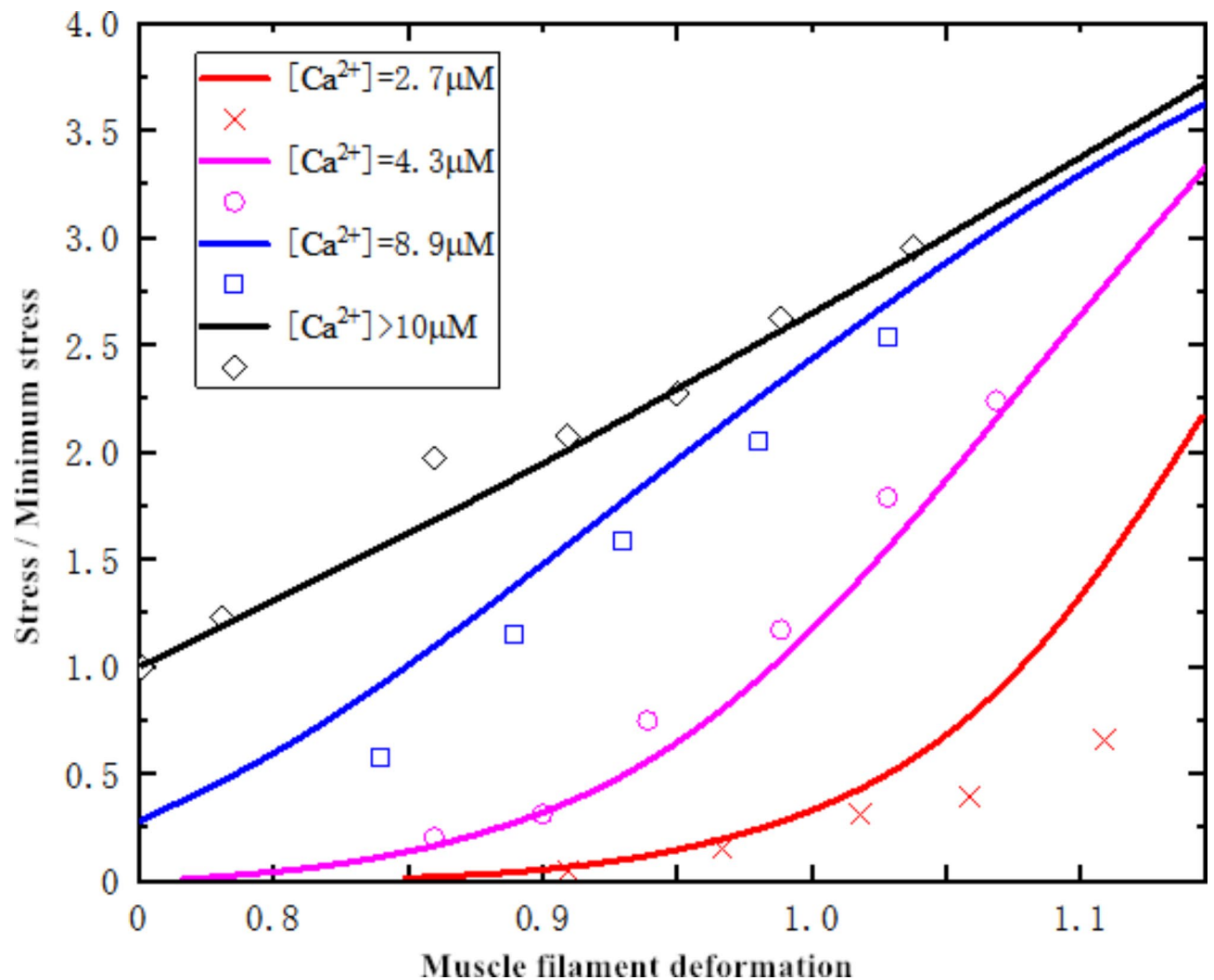


**Fig. 5.** Simulation results of stress-filament deformation relationship under different calcium ion concentrations.

and contraction speed was obtained. By comparing the results of classical experiments and similar models in literature, the validity and correctness of the multiscale model are verified.

In order to further improve the deficiency, it is necessary to study the relationship between calcium ions, muscle strength and muscle fatigue in the model. Only the synergistic effect of phosphate ions and muscle filaments in the process of contraction is considered, but the influence of anaerobic respiration and the change of muscle microstructure on the model is not considered. When the muscle strength reaches the maximum, the muscle strength no longer increases and starts to decline. Under different fatigue degrees, the peak value of muscle strength decreases with the increase of muscle fatigue. These results prove that the synergistic effect of phosphate and myofilament can affect the circulation of calcium ions, thus affecting muscle fatigue and muscle strength generation. The concentration of calcium ions in muscle fibers is transported in the sarcoplasmic reticulum and intersarcoplasmic to promote the circulation of the transverse bridge. When the concentration of calcium ions is constant, the muscle force increases with the growth of the myofilament deformation, and the growth rate is faster and faster. Under the same myofilament deformation, the higher the concentration of calcium ions, the greater the muscle force, but when the concentration of calcium ions reaches a certain threshold, the muscle force no longer increases, reflecting the microscopic mechanism of calcium ions to promote the generation of muscle force. Meanwhile, through the comparison of simulation results, it is proved that the synergistic effect of myofilament affects the circulation movement of the transverse bridge, thus affecting the generation of muscle force.

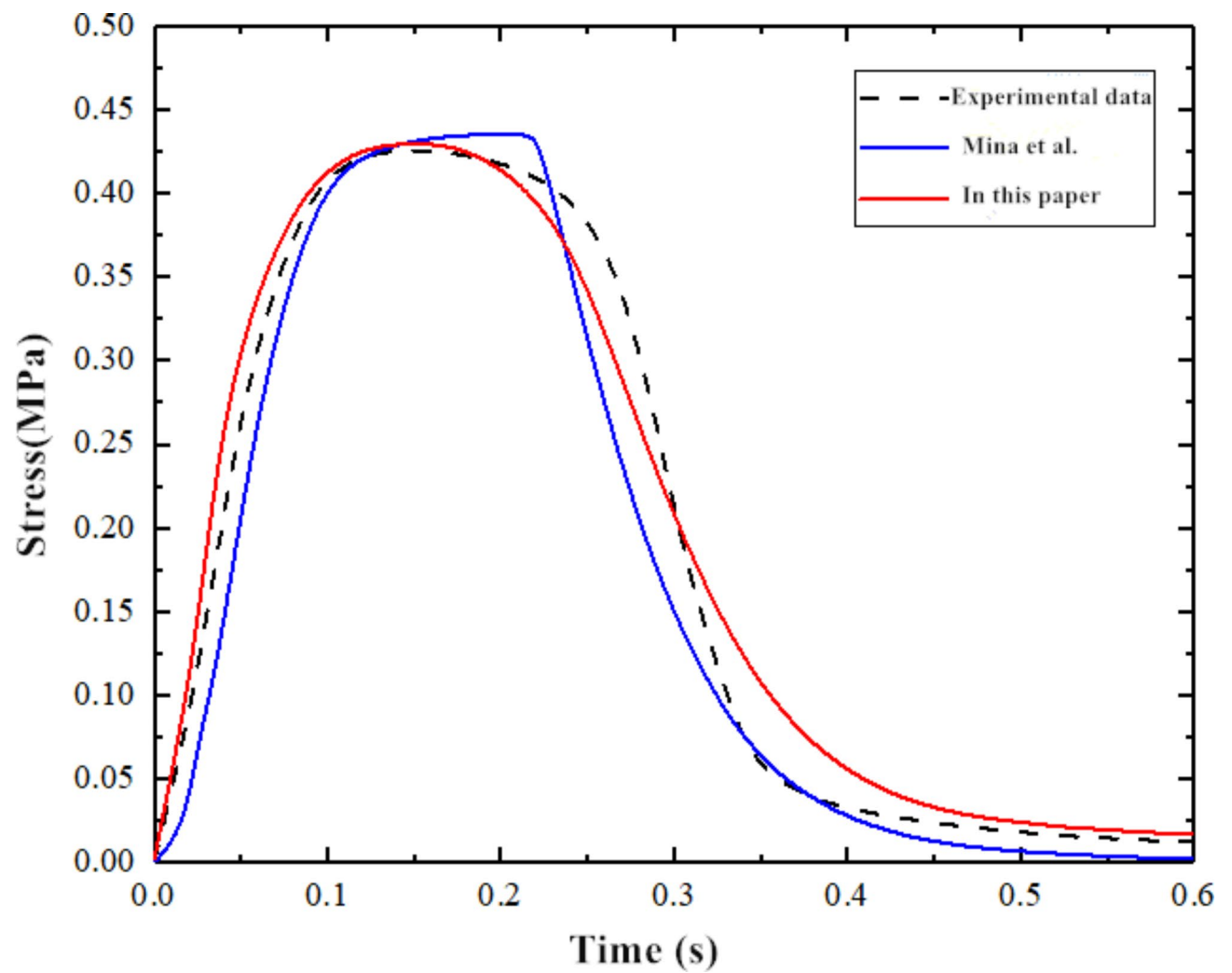


Fig. 6. Simulation results of skeletal muscle stress under non-fatigue condition.

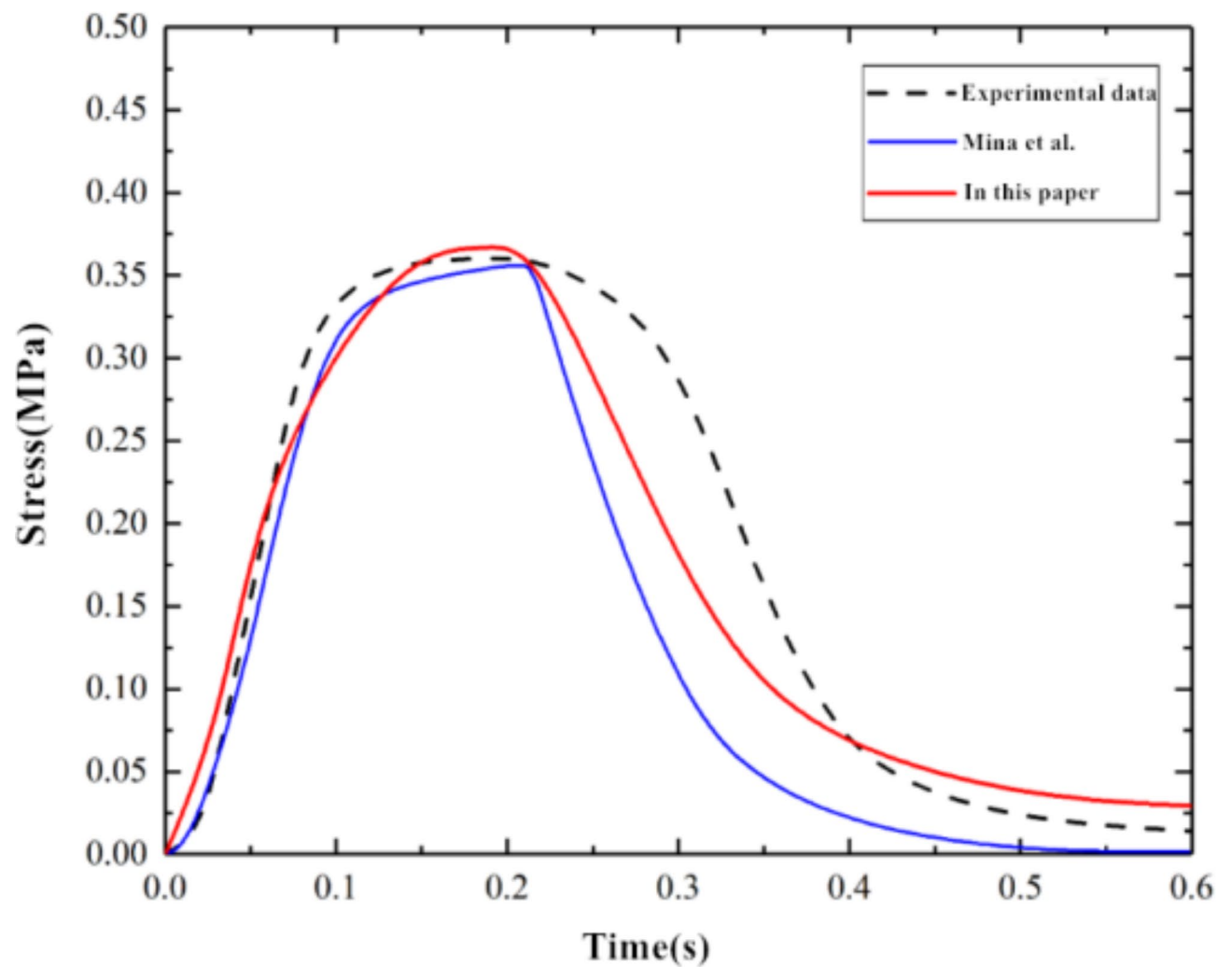
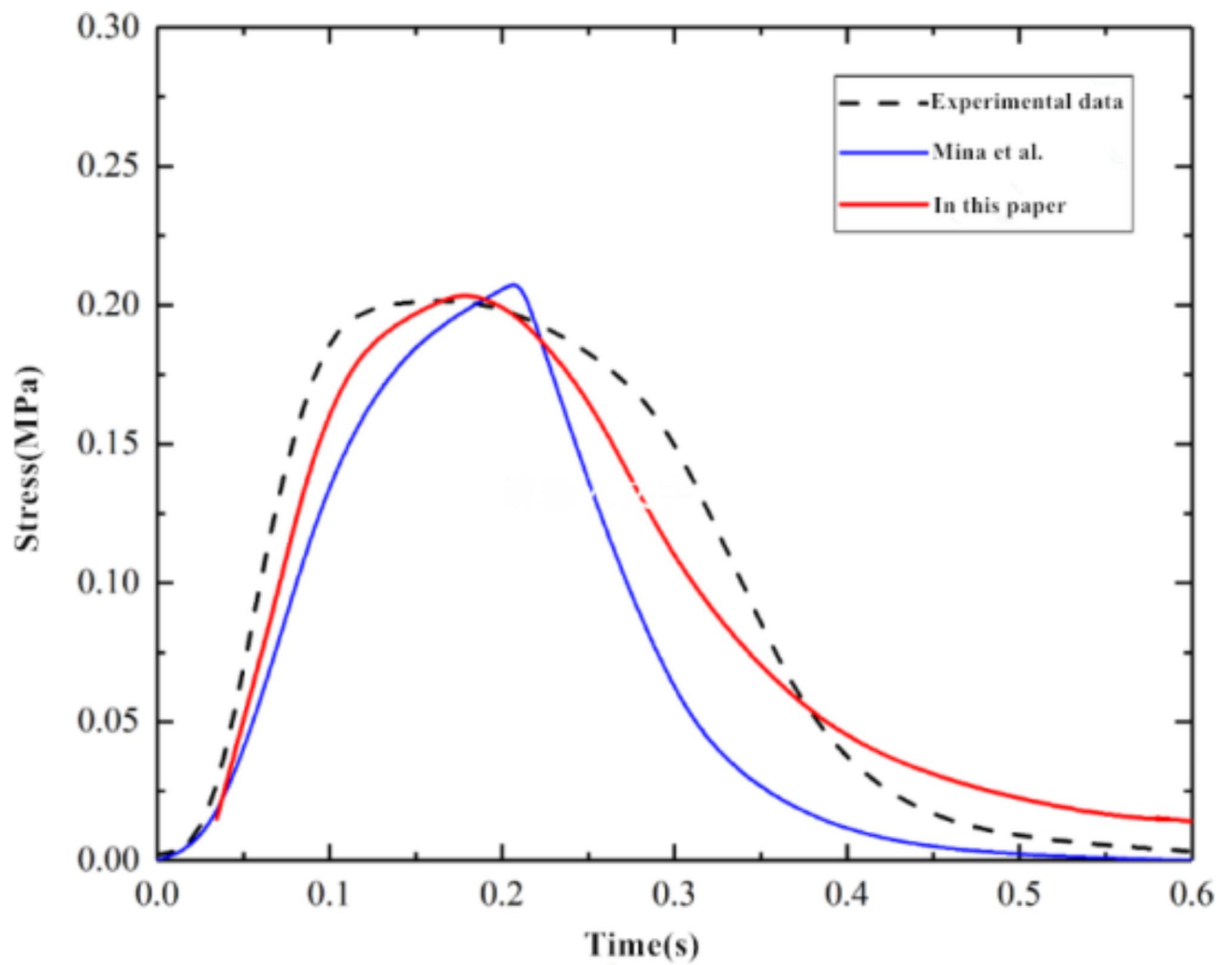
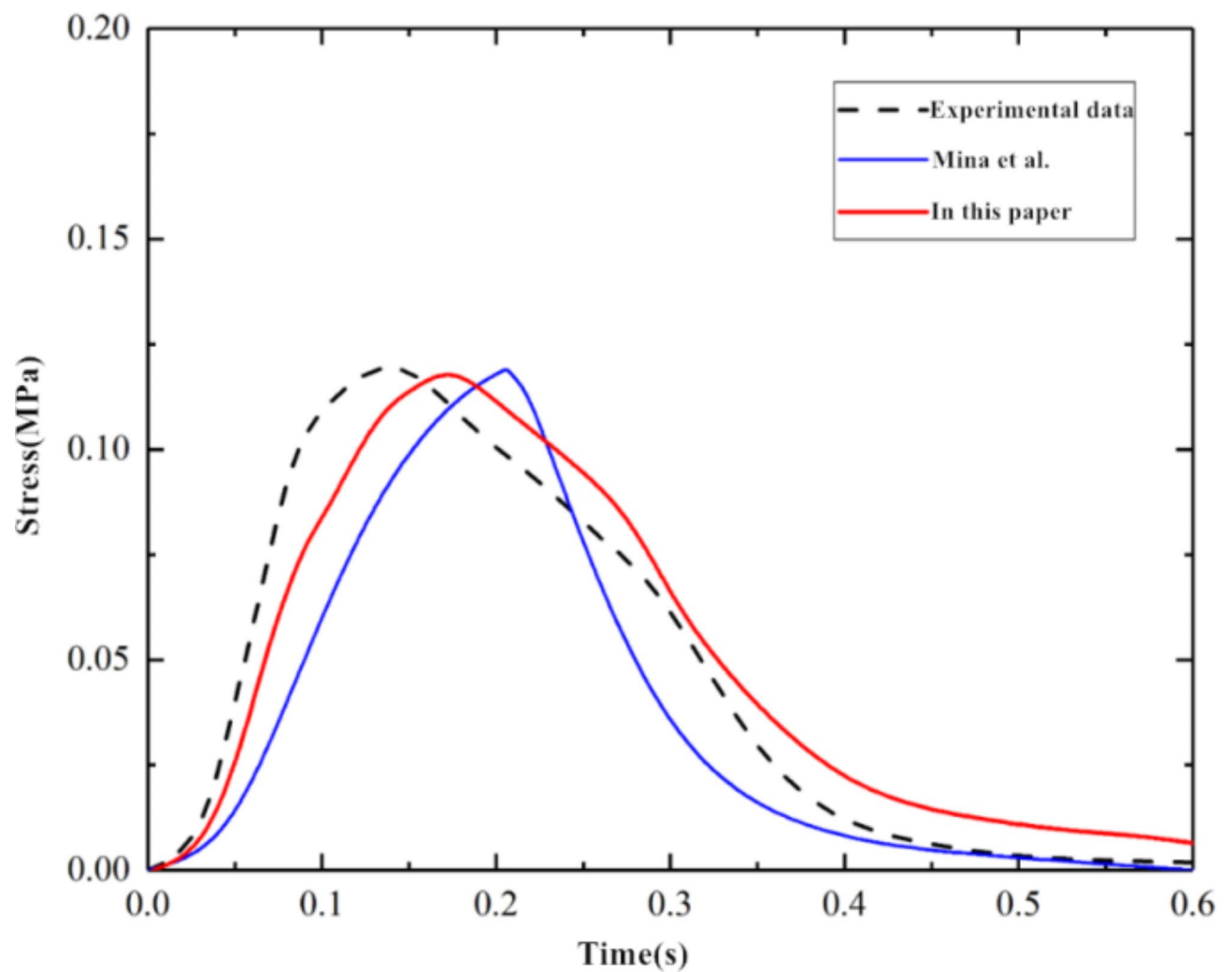


Fig. 7. Skeletal muscle stress changes under 16% fatigue.





**Fig. 8.** Skeletal muscle stress changes under 53% fatigue.



**Fig. 9.** Skeletal muscle stress changes under 72% fatigue.

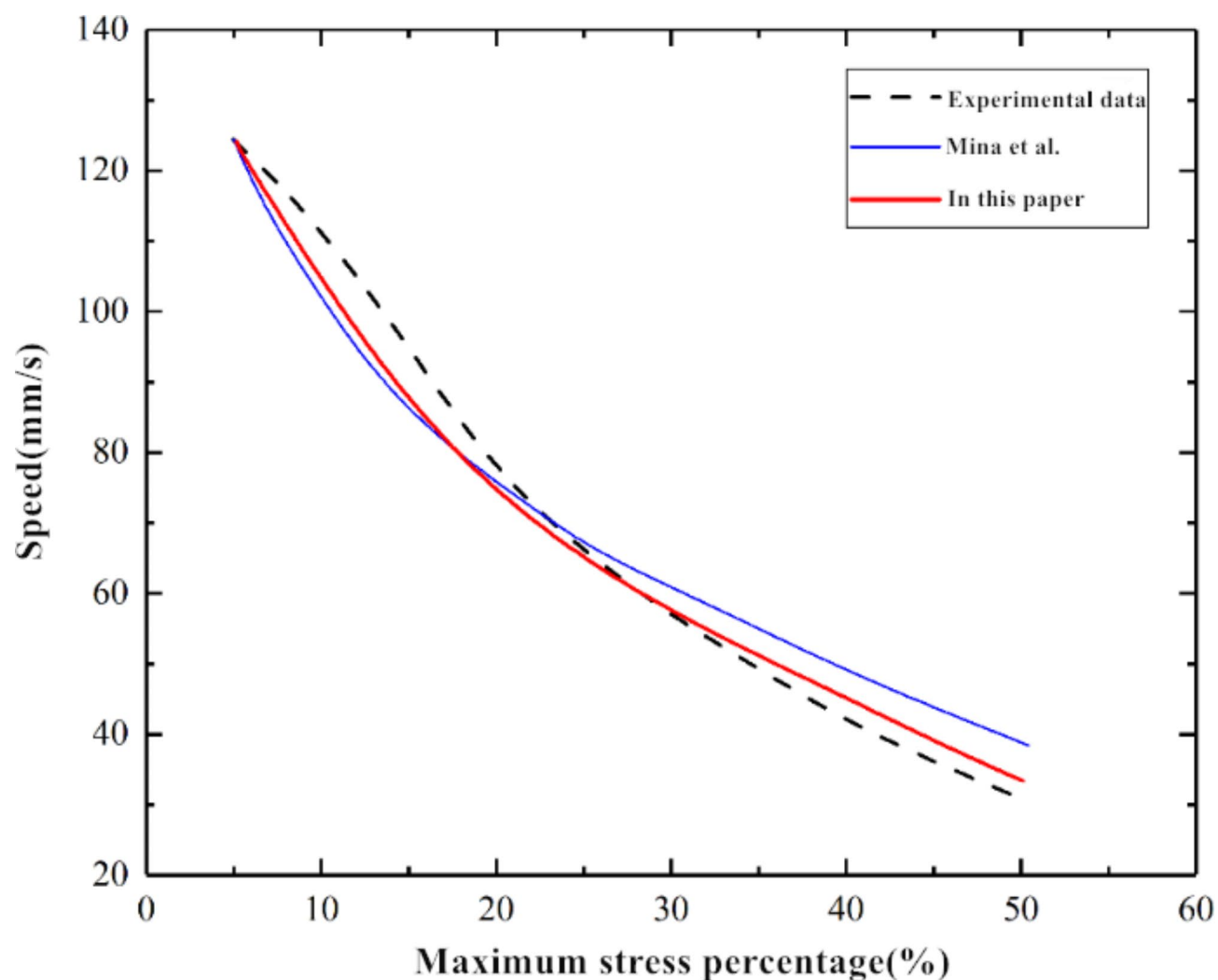


**Fig. 10.** Simulation results of skeletal muscle stress-contraction velocity relationship.

## Data availability

The datasets used and analysed during the current study available from the corresponding author on reasonable request.

Received: 16 July 2024; Accepted: 20 January 2025

Published online: 31 March 2025

## References

- Baumert, P. et al. Neuromuscular fatigue and recovery after strenuous exercise depends on skeletal muscle size and stem cell characteristics. *Sci. Rep.* **11**, 7733 (2021).
- Kuntamallappanavar, G., Toro, L., & Dopico, A. M. Both transmembrane domains of BK  $\beta 1$  subunits are essential to Confer the normal phenotype of  $\beta 1$ -Containing BK channels. *PLOS ONE* **9**(10), e109306 (2014).
- Oomens, C. W. J., Bader, D. L. & Loerakker, S. Baaijens. Pressure induced deep tissue injury explained. *Ann. Biomed. Eng.* **43**, 297–305 (2015).
- Walpole, J. & Papin, J. A. Peirce. Multiscale computational models of complex biological systems. *Annu. Rev. Biomed. Eng.* **15**, 137–154 (2013).
- Crampin, E. J., Smith, N. P. & Hunter, P. J. Multi-scale modelling and the IUPS physiome project. *J. Mol. Histol.* **35**, 707–714 (2004).
- Fenwick, A. J., Lin, D. C. & Tanner, B. C. W. Myosin cross-bridge kinetics slow at longer muscle lengths during isometric contractions in intact soleus from mice. *P Roy Soc. B-biol Sci.* **288**, 7–9 (2021).
- Maier, B. & Schulte, M. Mesh generation and multi-scale simulation of a contracting muscle–tendon complex. *J. Comput. Sci-neth.* **59**, 8–10 (2022).
- Villota-Narvaez, Y., Garzón-Alvarado, D. A. & Röhrle, O. Ramírez-Martínez. Multi-scale mechanobiological model for skeletal muscle hypertrophy. *Front. Physiol.* **13**, 10–12 (2022).
- Karamia, M., Zohoor, H., Calvo, B. & Grasa, J. A 3D multi-scale skeletal muscle model to predict active and passive responses. Application to intra-abdominal pressure prediction. *Comput. Method Appl. M.* **415**, 16–19 (2023).

10. Zhou, L., Liu, S. & Zheng, W. Automatic analysis of transverse Musculoskeletal Ultrasound images based on the Multi-task Learning Model. *Entropy-switz* **25**, 18 (2023).
11. Zhang, Mingxia., Zhao, Liangrun., Wang, Xiaohan. & Lo, Wai Leung Ambrose. et al. Automatic extraction and measurement of ultrasonic muscle morphological parameters based on multi-stage fusion and segmentation. *Clarivate Analytics Web Sci.* **137**, 107187(2024).
12. Maier, B., Göddeke, D. et al. OpenDiHu: an efficient and scalable framework for biophysical simulations of the neuromuscular system. *Clarivate Analytics Web Sci.* **79**, 102291 (2024).
13. Nna, B. et al. Biomimetic glycosaminoglycan-based scaffolds improve skeletal muscle regeneration in a murine volumetric muscle loss model. *Bioactive Mater.* **6**, 1201–1213 (2021).
14. Maleiner, B., Tomasch, J., Heher, P., Spadiut, O., Rünzler, D., & Fuchs, C. The importance of Biophysical and biochemical stimuli in dynamic skeletal muscle models. *Front. Physiol.* **9**, <https://doi.org/10.3389/fphys.2018.01130> (2018).
15. Julie, H. & Cieslar, G. P. Dobson, Free [ADP] and aerobic muscle work follow at least second order kinetics in rat gastrocnemius in vivo. *J. Biol. Chem.* **275** (9), 29–34 (2000).
16. Hunter, P. J. & McCulloch Keurs. Modelling the mechanical properties of cardiac muscle[J]. *Progress Biophys. Mol. Biology.* **69** (2), 289–331 (1998).
17. Sierra, M. et al. Predicting muscle fatigue: a response surface approximation based on proper generalized decomposition technique[J]. *Biomech. Model. Mechanobiology.* **16** (2), 1–10 (2016).
18. Shorten, P. R. et al. A mathematical model of fatigue in skeletal muscle force contraction. *J. Muscle Res. Cell. M.* **28**, 293–313 (2007).
19. Yoo, A. et al. Chrysanthemi Zawadzskii var. Latilobum attenuates obesity-Induced skeletal muscle atrophy via regulation of PRMTs in skeletal muscle of mice. *Int. J. Mol. Sci.* **21**, 16–29 (2020).
20. Bleiler, C. P. & Röhrle, O. A microstructurally-based, multi-scale, continuum-mechanical model for the passive behavior of skeletal muscle tissue. *J. Mech. Behav. Biomed. Mater.* **97**, 171–186 (2019).
21. Katrina, M. et al. Use it or lose it: multiscale skeletal muscle adaptation to mechanical stimuli. *Biomechanics and Modeling in Mechanobiology*, **14**(2), 195–215.(2015).
22. artori, M. & Yavuz, U. S. Farina. In vivo neuromechanics: decoding causal motor neuron behavior with resulting musculoskeletal function. *Sci. Rep.* **7**, 13465 (2017).
23. Fung, Y. C. *Biomechanics: Mechanical Properties of Living Tissues* (Springer-, 1981).
24. Farina, D., Muceli, S. & Enoka, R. M. Principles of motor unit physiology evolve with advances in technology. *J. Physiol.* **31**, 83–94 (2016).
25. Reyes-Villagrana, R. A. et al. High-intensity ultrasonication of rabbit carcasses: a first glance into a small-scale model to improve meat quality traits. *Ital. J. Anim. Sci.* **19**, 544–550 (2020).
26. Mueller, A. L. & Bloch, R. J. Skeletal muscle cell transplantation: models and methods. *J. Muscle Res. Cell. M.* **5**, 297–311 (2019).
27. Hill, A. V. The maximum work and mechanical efficiency of human muscles, and their most economical speed. *J. Physiol.* **56**, 19–41 (1922).
28. Hill, A. V. The heat of shortening and the dynamic constants of muscle. *P Roy Soc.* **126**, 136–195 (1938).
29. Chokhandre, S., Colbrunn, R., Bennetts, C. & Erdemir, A. A comprehensive specimen-specific multiscale data set for anatomical and mechanical characterization of the tibiofemoral joint. *PLoS ONE*. **10**, e0138226 (2015).
30. Shorten, P. R., O'Callaghan, P., Davidson, J. B. & Soboleva, T. K. A mathematical model of fatigue in skeletal muscle force contraction. *J. Muscle Res. Cell. Motil.* **28**, 293–313 (2007).
31. Choi, H. F., Chincisan, A., Becker, M. & Magnenat-Thalmann, N. Multimodal composition of the digital patient: a strategy for the knee articulation. *Visual Comput.* **30**, 739–749 (2014).
32. Hunter, P., Smith, N. & Fernandez, J. Integration from proteins to organs: the IUPS Physiome Project. *Mech. Ageing Dev.* **126**, 187–192 (2005).
33. Logsdon, E. A., Finley, S. D., Popel, A. S. & Mac Gabhann, F. A systems biology view of blood vessel growth and remodelling. *J. Cell. Mol. Med.* **18**, 1491–1508 (2014).
34. Murfee, W. L., Sweat, R. S., Tsubota, K., Mac Gabhann, F. & Khismatullin, D. Peirce. Applications of computational models to better understand microvascular remodelling: a focus on biomechanical integration across scales. *Interface Focus.* **5**, 20140077 (2015).
35. Lanir, Y. Multi-scale Structural Modeling of Soft Tissues Mechanics and mechanobiology. *J. Elast.* **129**, 7–48 (2017).
36. Tawhai, M. H. & Bates, J. H. Multi-scale lung modeling. *J. Appl. Physiol.* **110**, 1466–1472 (2011).
37. Nickerson, D. P., Terkildsen, J. R. & Hamilton, K. L. Hunter. A tool for multi-scale modelling of the renal nephron. *Interface Focus.* **1**, 417–425 (2011).
38. Greenstein, J. L. & Winslow, R. L. Integrative systems models of cardiac excitation-contraction coupling. *Circ. Res.* **108**, 70–84 (2011).
39. Syomin, F. A. & Tsaturyan, A. K. A simple model of cardiac muscle for multiscale simulation: Passive mechanics, crossbridge kinetics and calcium regulation. *J. Theor. Biol.* **420**, 105–116 (2017).
40. Ren, L., Qian, Z. & Ren, L. Biomechanics of musculoskeletal system and its biomimetic implications: a review. *J. Bionic Eng.* **11**, 159–175 (2014).
41. Ivanovic, M., Stojanovic, B., Kaplarevic-Malisic, A., Gilbert, R. & Mijailovich, S. Distributed multi-scale muscle simulation in a hybrid MPI-CUDA computational environment. *Simul. - T Soc. Mod. Sim.* **92**, 19–31 (2005).
42. Korzeniewski, B. & Zoladz, J. A. A model of oxidative phosphorylation in mammalian skeletal muscle[J]. *Biophys. Chem.* **92** (1), 17–34 (2001).
43. Korzeniewski, B. & Anderson, R. M. Regulation of oxidative phosphorylation is different in electrically- and cortically-stimulated skeletal muscle[J]. *Plos One.* **13** (4), 69–82 (2018).
44. Benoussaad, M. et al. Synthesis of optimal electrical stimulation patterns for functional motion restoration: applied to spinal cord-injured patients. *Med. Biol. Eng. Comput.* **53**, 227–243 (2015).
45. Fernandez, J. et al. D.Lloyd. Multiscale musculoskeletal modelling, data-model fusion and electromyography-informed modelling. *Interface Focus.* **6**, 20150084 (2016).
46. Mijailovich, S. M. et al. Three-dimensional stochastic model of actin-myosin binding in the sarcomere lattice. *J. Gen. Physiol.* **148**, 459–488 (2016).
47. Zajac, F. E. Muscle and tendon: Properties, models, scaling, and application to biomechanics and motor control. *Crit. Rev. Biomed. Eng.* **17**, 359–411 (1989).
48. Stoecker, U., Telley, I. A., Stüssi, E. & Denoth, J. A multisegmental cross-bridge kinetics model of the myofibril. *J. Theor. Biol.* **259**, 714–726 (2009).
49. Denoth, J., Stüssi, E., Csucs, G. & Danuser, G. Single muscle fiber contraction is dictated by inter-sarcomere dynamics. *J. Theor. Biol.* **216**, 101–122 (2002).
50. Prado, L. G. et al. Isoform diversity of giant proteins in relation to passive and active contractile properties of rabbit skeletal muscles. *J. Gen. Physiol.* **126**, 461–480 (2005).
51. Huijing, P. A. Muscle as a collagen fiber reinforced composite: a review of force transmission in muscle and whole limb. *J. Biomech.* **32**, 329–345 (1999).
52. Blemker, S. S. & Delp, S. L. Three-dimensional representation of complex muscle architectures and geometries. *Ann. Biomed. Eng.* **35**, 661–673 (2015).

53. Röhrle, O. & Pullan, A. J. Three-dimensional finite element modelling of muscle forces during mastication. *J. Biomech.* **40**, 3363–3372 (2016).
54. Ramasamy, E., Avci, O. & Dorow, B. An efficient modelling-simulation- analysis workflow to investigate stump-socket interaction using patient-specific, three-dimensional, continuum-mechanical, finite element residual limb models. *Front. Bioeng. Biotech.* **6**, 126–126 (2018).
55. Huxley, A. F. Muscle structure and theories of contraction. *Prog Biochem. Biophys.* **7**, 255–318 (1957).
56. Huxley, H. E. & Hanson, J. Changes in the cross-striations of muscle during contraction and stretch and their structural interpretation. *Nature* **173**, 973–976 (1954).
57. Huxley, A. F. & Niedergerke, R. Structural changes in muscle during contraction: interference microscopy of living muscle fibers. *Nature* **173**, 971–973 (1954).
58. Leeuwen, J. L. V. Optimum power output and structural design of sarcomeres. *J. Theor. Biol.* **149**, 229–256 (1991).
59. Adrian, R. H. & Peachey, L. D. Reconstruction of the action potential of frog Sartorius muscle. *J. Physiol.* **235**, 103–131 (1973).
60. Wallinga, W. et al. Modelling action potentials and membrane currents of mammalian skeletal muscle fibers in coherence with potassium concentration changes in the T-tubular system. *Eur. Biophys. J.* **28**, 317–329 (1999).
61. Cannon, S. C., Brown, R. H. & Corey, D. P. Theoretical reconstruction of myotonia and paralysis caused by incomplete inactivation of sodium channels. *Biophys. J.* **65**, 270–288 (1993).
62. Smith, N. P., Barclay, C. J. & Loisel, D. S. The efficiency of muscle contraction. *Prog Biophys. Mol. Bio.* **88**, 1–58 (2005).
63. Cannell, M. B. & Allen, D. G. Model of calcium movements during activation in the sarcomere of frog skeletal muscle. *Biophys. J.* **45**, 913–925 (1984).
64. Pizarro, G. & Olivera, J. F. The dynamics of Ca<sup>2+</sup> within the sarcoplasmic reticulum of frog skeletal muscle. A simulation study[J]. *J. Theor. Biol.* **504** (2), 11–37 (2020).
65. Gillis, J. M., Thomason, D., Lefèvre, J. & Kretzinger, R. Parvalbumins and muscle relaxation: a computer simulation study. *J. Muscle Res. Cell. M.* **3**, 377–398 (1982).
66. Baylor, S. M. & Hollingworth, S. Model of Sarcomeric Ca<sup>2+</sup> movements, including ATP Ca<sup>2+</sup> binding and diffusion, during activation of frog skeletal muscle. *J. Gen. Physiol.* **112**, 297–316 (1998).
67. Bradley, C. P. et al. Enabling detailed, Biophysics-based skeletal muscle models on HPC System. *Front. Physiol.* **9**, 816–825 (2018).
68. Bhattacharya, P. & Viceconti, M. Multiscale modelling methods in biomechanics. *Wires Syst. Biol. Med.* **9**, e1375 (2017).
69. Röhrle, O. et al. Bridging scales: a three-dimensional electromechanical finite element model of skeletal muscle. *Siam J. Sci. Comput.* **30**, 2882–2904 (2008).
70. Kin, J. H., Trew, M. L., Pullan, A. J. & Röhrle, O. Simulating a dual-array electrode configuration to investigate the influence of skeletal muscle fatigue following functional electrical stimulation. *Comput. Biol. Med.* **42**, 915–924 (2012).
71. Virgilio, K. M., Peirce, S. M. & Blemker, S. S. Multiscale models of skeletal muscle reveal the complex effects of muscular dystrophy on tissue mechanics and damage susceptibility. *Interface Focus* **5**, 1–10 (2015).
72. Schröder, J. et al. A numerical two-scale homogenization scheme: The FE2-method. *Plasticity and beyond, volume 550 of CISM international center for mechanical sciences.* **8**, 1–64 (2014).
73. Hernández-Gascón, B., Calvo, B. & Rodríguez, J. F. A 3D electro-mechanical continuum model for simulating skeletal muscle contraction. *J. Theor. Biol.* **335**, 108–118 (2013).
74. Böl, M., Weikert, R. & Weichert, C. A coupled electromechanical model for the excitation-dependent contraction of skeletal muscle. *J. Mech. Behav. Biomed.* **4**, 1299–1310 (2011).

## Acknowledgements

The work described in this study was supported in part by National Natural Science Foundation of China(No.61972117).

## Author contributions

Monan Wang defined the research problem and designed the research idea, Daixin Jin completed the article layout、 submission and result analysis, Haibin Wang completed the modeling and simulation, Xinyi Xu and Siyuan Zheng completed the article was organized, translated, and revised, Juntong Jing completed the article translated and revised.All authors reviewed the manuscript.

## Declarations

## Competing interests

The authors declare no competing interests.

## Additional information

**Correspondence** and requests for materials should be addressed to M.W.

**Reprints and permissions information** is available at [www.nature.com/reprints](http://www.nature.com/reprints).

**Publisher's note** Springer Nature remains neutral with regard to jurisdictional claims in published maps and institutional affiliations.

**Open Access** This article is licensed under a Creative Commons Attribution-NonCommercial-NoDerivatives 4.0 International License, which permits any non-commercial use, sharing, distribution and reproduction in any medium or format, as long as you give appropriate credit to the original author(s) and the source, provide a link to the Creative Commons licence, and indicate if you modified the licensed material. You do not have permission under this licence to share adapted material derived from this article or parts of it. The images or other third party material in this article are included in the article's Creative Commons licence, unless indicated otherwise in a credit line to the material. If material is not included in the article's Creative Commons licence and your intended use is not permitted by statutory regulation or exceeds the permitted use, you will need to obtain permission directly from the copyright holder. To view a copy of this licence, visit <http://creativecommons.org/licenses/by-nc-nd/4.0/>.

© The Author(s) 2025